



# Thermo-economic modeling of an indirectly coupled solid oxide fuel cell/gas turbine hybrid power plant

Denver F. Cheddie<sup>a,\*</sup>, Renique Murray<sup>b</sup>

<sup>a</sup> Center for Energy Studies, University of Trinidad and Tobago, Point Lisas Campus, Esperanza Road, Brechin Castle, Couva, Trinidad and Tobago

<sup>b</sup> Natural Gas Institute of the Americas, University of Trinidad and Tobago, Point Lisas Campus, Esperanza Road, Brechin Castle, Couva, Trinidad and Tobago

## ARTICLE INFO

### Article history:

Received 4 June 2010

Received in revised form 5 July 2010

Accepted 6 July 2010

Available online 13 July 2010

### Keywords:

Thermo-economic model

Solid oxide fuel cell

Gas turbine

Indirect coupling

## ABSTRACT

Power generation using gas turbine (GT) power plants operating on the Brayton cycle suffers from low efficiencies, resulting in poor fuel to power conversion. A solid oxide fuel cell (SOFC) is proposed for integration into a 10 MW gas turbine power plant, operating at 30% efficiency, in order to improve system efficiencies and economics. The SOFC system is indirectly coupled to the gas turbine power plant, paying careful attention to minimize the disruption to the GT operation. A thermo-economic model is developed for the hybrid power plant, and predicts an optimized power output of 20.6 MW at 49.9% efficiency. The model also predicts a break-even per-unit energy cost of USD 4.65  $\text{¢ kWh}^{-1}$  for the hybrid system based on futuristic mass generation SOFC costs. This shows that SOFCs may be indirectly integrated into existing GT power systems to improve their thermodynamic and economic performance.

© 2010 Elsevier B.V. All rights reserved.

## 1. Introduction

Fuel cells are electrochemical devices that convert the chemical energy in a fuel into electricity without direct combustion. As a result, they avoid many of the limitations of combustion engines, providing more energetically and exergetically efficient fuel to power conversion. Solid oxide fuel cells (SOFCs) are best suited for distributed power generation. They operate at temperatures between 600 and 1100 °C and have been tested at operating pressures up to 15 atm [1]. Because of their high temperature and pressure exhaust, SOFCs are considered ideal for integration in hybrid power generating systems, where they are coupled with gas turbines (GT) to produce additional power.

SOFC hybrid power systems have received considerable interest in the literature over the past 5–10 years. Zhang et al. [2] gave a comprehensive list of strategies for integrating SOFCs with other power generating components. These schemes can be categorized as direct thermal coupling, indirect thermal coupling, and fuel coupling. Direct thermal coupling involves two or more power systems (e.g. SOFC and GT) sharing the same working fluid. In indirect ther-

mal coupling, different working fluids are kept separate; only heat is transferred between the two power systems via heat exchangers. Fuel coupling schemes involve the configuring of the integration system to include hydrogen production or fuel reforming.

There are only a few prototype hybrid power plants in existence [3–5], primarily because of the prohibitive cost of SOFC technology, so researchers resort to mathematical modeling to predict the performance of hybrid power plants. Massardo and Lubelli [6] developed a thermodynamic model for a multi-MW demonstration plant based on an internally reforming SOFC and gas turbine cycles. Chan et al. [7] added an exergy analysis to a SOFC model, a concept which was later incorporated into hybrid plant models [8–14]. Akkaya et al. [14] introduced an exergetic performance coefficient to quantify the second law thermodynamic performance of the hybrid plant, and allowed for easy identification of the chief sources of exergy destruction in the plant. Burbank et al. [15] considered a pressurized SOFC–GT engine which entailed a variable geometry nozzle turbine to directly influence the airflow as well as an auxiliary combustor to control the temperature of turbomachinery. Song et al. [10] and Calise et al. [16] modeled part load operating conditions of hybrid plants. Both found that the best control strategy for part load operation was simultaneously varying the air and fuel flow rates while maintaining a constant air/fuel ratio. This was necessary to keep the SOFC and GT operating as close to their design temperatures at all times. Franzoni et al. [17] modeled a plant which considered carbon dioxide separation, enabled by condensing the turbine exhaust stream.

Abbreviations: AB, after burner; AC, air compressor; FC, fuel compressor; GT, gas turbine; HX, heat exchanger; MX, mixer; NPV, net present value (USD); PR, pre-reformer; SOFC, solid oxide fuel cell.

\* Corresponding author. Tel.: +868 343 5014; fax: +868 636 3339.

E-mail addresses: [denver.cheddie@utt.edu.tt](mailto:denver.cheddie@utt.edu.tt), [dcheddie@yahoo.com](mailto:dcheddie@yahoo.com) (D.F. Cheddie).

### Nomenclature

$A$	area ( $\text{m}^2$ )
$C$	cost (USD)
$e$	standard chemical exergy ( $\text{J mol}^{-1}$ )
$E$	potential (V)
$F$	Faraday constant ( $96,485 \text{ C mol}^{-1}$ )
$H$	enthalpy (W)
$h$	molar enthalpy ( $\text{J mol}^{-1}$ )
$i$	current density ( $\text{A m}^{-2}$ )
$I$	irreversibility (W)
$N$	molar flow rate ( $\text{mol s}^{-1}$ )
$p$	pressure (Pa)
$P$	power (W)
$Q$	heat (W)
$R$	universal gas constant ( $8.3143 \text{ J mol}^{-1} \text{ K}^{-1}$ )
$S$	entropy ( $\text{W K}^{-1}$ )
$s$	molar entropy ( $\text{J mol}^{-1} \text{ K}^{-1}$ )
$T$	temperature (K)
$U$	utilization factor
$V$	potential (V)
$W$	work (W)
$x$	mole ratio of methane to oxygen
$\eta$	efficiency (%), overpotential (V)
$\psi$	exergy (W)

Economic studies have also been conducted on SOFC hybrid power systems. Palazzi et al. [18] discussed thermo-economic optimization techniques using pinch based methods. Arsalis [19] performed a detailed thermo-economic assessment of a 1.5–10 MWe hybrid system. Santin et al. [20] considered the use of liquid fuels (methanol and kerosene) instead of methane/natural gas primarily because of their ease of transport. For a 500 kW plant, they found that the use of methanol instead of methane reduced the plant efficiency by up to 7%, however, reduced the payback period on the investment by 0.5 years. This was because of the lower capital cost associated with handling methanol.

The goal of thermo-economic analyses is to maximum system efficiencies, minimize irreversibilities or maximize the cost benefit. Various optimization techniques have been presented in the literature. Single-level modeling aims to optimize the entire system as a whole [21], while multi-level modeling seeks to simultaneously optimize multiple subsystems [22,23]. Calise et al. [21] argue that single-level optimization produces similar results to multi-level efforts with less difficulty.

Although most of the literature thus far has been devoted to steady state analysis, dynamic modeling has also been attempted. Zhang et al. [24] modeled the dynamic performance of the SOFC on the basis of exponential decay and exponential associate functions. Kandepu et al. [25] developed a dynamic model based on lumped capacitance modeling and mass and energy conservation. However, most dynamic models focus on the SOFC rather than the entire power plant.

A wide scale of operation ranging from kW to MW has been considered in the literature. Most existing SOFC–GT hybrid plants are in the kW range [3–5], however, larger plants have been modeled in the literature. Chan et al. [22] considered a 1.3 MW plant, which consisted of a SOFC stack with 40,000 tubular cells. Arsalis [19] considered SOFC stacks up to 8.5 MW for a SOFC–GT–ST hybrid system. Their SOFC stack was modeled up to 1100 °C and 10 bar. They propose a system of this magnitude to provide distributed power for 2000 households. Their thermo-economic analysis showed that using a larger size SOFC results in better thermodynamic performance, but add significantly to the system costs since the SOFC

cost dominates the capital cost in hybrid systems. They also discussed the inherent difficulty in selecting a micro-gas turbine for small scale operation since their efficiencies decrease as the system scales down. One of the advantages of large scale operation is that, in theory, SOFC technology can easily be scaled up by adding more stacks. However, there are practical hurdles that must be overcome, such as localized hotspots and unbalanced loading on each stack. Singhal and Kendall [26] and Larminie and Dicks [27] predict that practical SOFC systems will be scaled up from 100 kW to 10 MW prior to commercialization of the technology [21].

Most of the SOFC–GT schemes presented in the literature involve direct thermal coupling. This is because the focus has been on designing new micro-power plants for small scale distributed power generation (<1 MW). However, there are GT power plants already in existence that operate at relatively low efficiencies. These power plants can be retrofitted using SOFC technology to improve their performance. In such cases, special care has to be taken to ensure that the addition of the SOFC system does not interfere with the operation of the GT power plant. For this reason, indirect coupling may be more feasible for such applications. Further, the existing GT power plants in question are larger in scale than those presently used in SOFC–GT hybrids, and thus would require larger scale SOFCs for effective coupling.

In this work, a 10 MW gas turbine power plant is considered, which entails a compression ratio of 10 and a turbine inlet temperature of 1400 K. A thermo-economic model is developed for an indirectly coupled hybrid system. The goal is to optimally size the SOFC stack to obtain the most cost effective performance of the system, and to study the behavior of the proposed system. It is assumed for the purposes of this work that in the future, the technology will become sufficiently mature that commercially available SOFCs would be in the 10 MW range.

## 2. Model development

### 2.1. Schematic

The existing power plant (hereafter referred to as the standard plant) is based on the standard Brayton cycle using natural gas to provide heat input. In this paper, natural gas is considered to be mostly methane with other components providing negligible contribution. It utilizes a compression ratio of 10, followed by combustion of natural gas (methane) to provide sufficient heat to achieve a turbine inlet temperature of 1400 K. The products of combustion are then expanded in the turbine back down to atmospheric pressure. Methane is consumed at a rate of  $40.0 \text{ kg min}^{-1}$  in the combustion processes. The isentropic efficiencies (82.3% and 86.0% for the compressor and turbine, respectively) and combustion efficiency (98.9%) are calculated from experimental data. At the time the measurements were taken, the plant was operating at full load, producing 10.0 MW of net power at a thermal efficiency of 30.0% and second law thermodynamic efficiency of 28.9%. This plant produces power at a break-even cost of  $5.46 \text{ ¢ kWh}^{-1}$ . The exergy breakdown for this standard plant is shown in Table 1. As expected, the combustion processes are largely

**Table 1**  
Exergy destruction in the standard and hybrid plants, MW (% of total power).

Process	Standard plant	Hybrid plant
Combustion	11.1 (111.2%)	4.26 (20.7%)
Fuel cell	NA	3.95 (19.2%)
Compression	1.1 (10.8%)	1.05 (5.1%)
Expansion	1.3 (12.7%)	1.25 (6.1%)
Heat exchange/mixing	NA	4.11 (20.1%)
Total exergy destruction	13.5 (134.7%)	14.62 (71.1%)
Total plant power	10.0	20.56

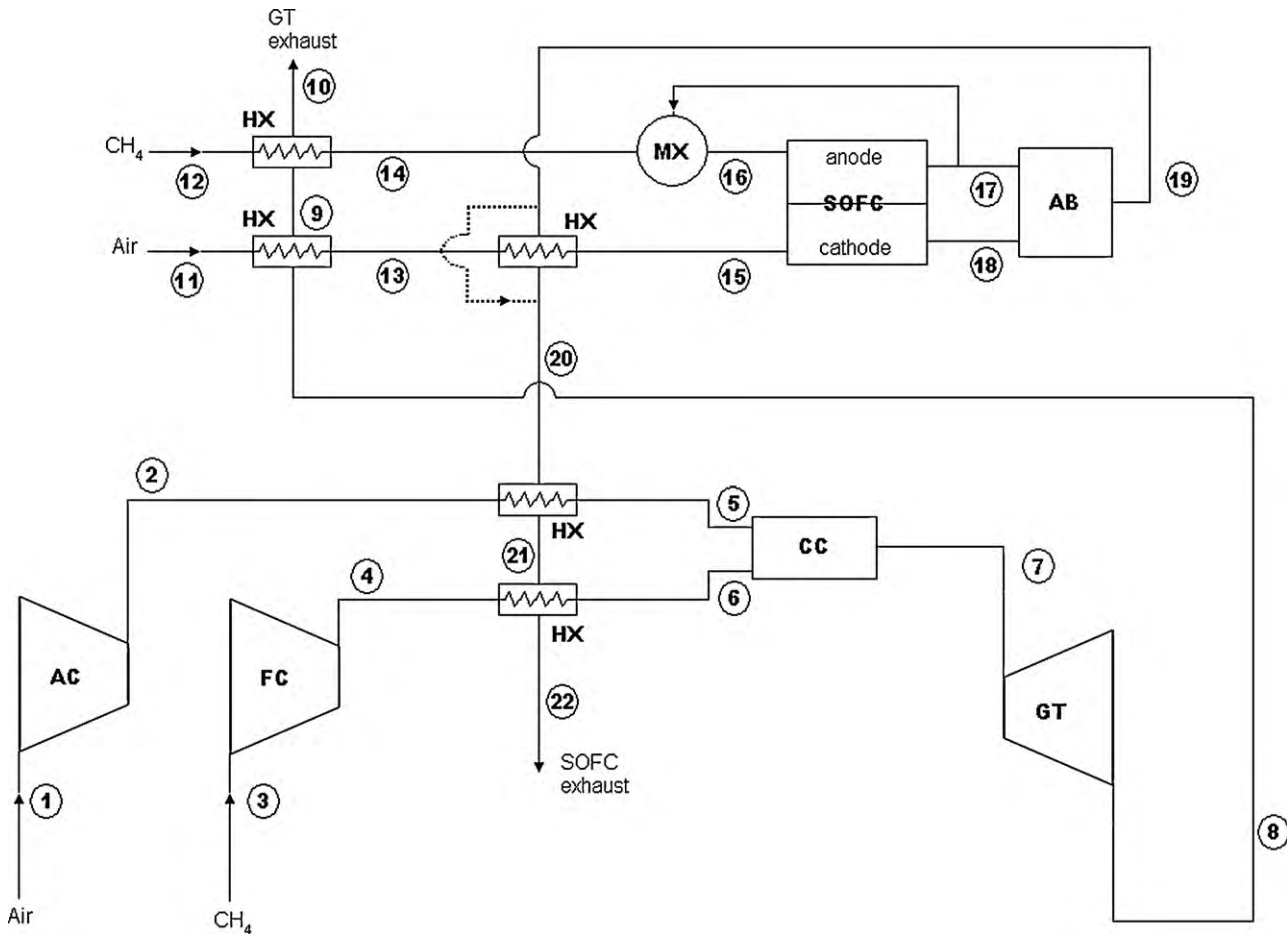


Fig. 1. Hybrid schematic using indirect coupling with anode recycle.

responsible for the large amounts of exergy destruction in such plants.

Fig. 1 shows the proposed hybrid configuration that is aimed at improving the thermodynamic and economic performance of the power plant. In this configuration, the goal is to couple the SOFC to the gas turbine power plant in a way that minimizes the disruption to normal operation. The fuel cell and the gas turbine operate with different fluid streams and thus would be characterized as indirect coupling. The outlet from the turbine is used to preheat the fuel cell reactants, while the outlet from the fuel cell is used to preheat the compressed gases entering the turbine. Preheating the fuel cell inlet gases results in a higher fuel cell operating temperature, and hence better performance. In addition, no external water is supplied to the fuel cell. Instead, a fraction of the anode outlet is recycled to provide steam for reformation of the methane. The amount of fuel supplied to the turbine is selected so as to maintain a turbine inlet temperature of 1400 K, thus preheating the turbine inlet gases reduces the amount of combustion required in the GT power plant. So this way, the SOFC and GT improve each others' performance.

Westinghouse tubular SOFC systems are considered in this paper. Since the fuel cell does not operate at 100% fuel utilization, an afterburner is still needed to combust excess fuel. The output from the afterburner is then used to preheat the air entering the fuel cell. This heat exchanger is equipped with a control mechanism that regulates the flow rates such that the SOFC temperature is maintained at 1373 K. In this work, the cell voltage is externally controlled and maintained at 0.5 V, while the current depends on the IV curve. The recycle fraction of the anode outlet is maintained at 0.6. Thus the fuel utilization factor is not a fixed parameter of the

SOFC, but can only be regulated by adjusting the fuel supply rate. Ideally the flow rates should be set such that 75% fuel utilization is observed.

## 2.2. Assumptions

Steady state full load conditions are studied in this paper. The schematic shown in Fig. 1 applies for full load operating point conditions. There are numerous practical contingencies that are deliberately not shown to avoid complicating the figure. For example, typically a stream from the air compressor is bled to the turbine inlet stream as a control mechanism to prevent the turbine inlet temperature from exceeding 1400 K. However, at the designed operating conditions, this flow will be zero. This ideal design condition is represented in Fig. 1. These contingencies are understood, but not shown.

Full combustion is also assumed. Combustion efficiency is taken to mean that 100% oxidation of the fuel occurs, however, some of the heat of combustion is "lost" to the environment. It is also assumed for convenience that all the heat losses in the plant take place in the combustion device. All other components are considered to be insulated from the environment.

Direct internal reforming SOFCs are considered in this paper, however, the thermodynamic analysis would still apply if an external reformer was used since the thermodynamic analysis of the fuel cell presented in this paper applies to the entire fuel cell system. The only factor that would be affected is the additional capital cost. It is also assumed that complete reformation of methane takes place in the reforming section of the SOFC, and that only hydrogen, carbon dioxide and water vapor exist in the anode section of the SOFC.

### 2.3. Equations

In this work, a lumped approach is used to analyze each component of the plant. Mass and energy balances are considered across each component, the first and second laws of thermodynamics are applied to determine outlet states and exergy destruction:

$$Q - W = \Delta H \quad (1)$$

The total exergy (physical + chemical) for each component  $i$  is given by Eq. (2), where  $e^0$  is the standard chemical exergy for each substance [28]:

$$\psi_i = (h_i - h_{i,0}) - T_0(s_i - s_{i,0}) + e_i^0 + RT_0 \ln(x_i) \quad (2)$$

The first law thermodynamic efficiency is defined as the ratio of net electrical power output to total heat input. The second law thermodynamic efficiency is defined as the ratio of net power output to the total exergy input. The enthalpy and entropy values of each gas species are determined from coefficients used in Ref. [29]:

$$\eta_I = \frac{W_{net}}{Q_{in}} \quad (3)$$

$$\eta_{II} = \frac{W_{net}}{Ex_{in}} \quad (4)$$

#### 2.3.1. Combustor, mixer and heat exchangers

In the combustion chamber, no work is done and only the heat losses to the environment need to be considered. The heat of reaction is already incorporated in the outlet enthalpy values. The outlet composition is determined from a molar balance assuming complete combustion of methane and hydrogen. Excess air is assumed to ensure complete combustion:



For known inlet conditions, the combustion outlet temperature is determined so as to ensure Eq. (1) is satisfied. An iterative approach based on the Newton-Raphson method, is used in this work to accomplish this goal:

$$\sum (n_i h_i^T)_{out} = -Q_{loss} + \sum (n_i h_i^T)_{in} \quad (7)$$

Mixing processes are treated in an identical manner, except that the outlet composition is merely the algebraic sum of all inlet compositions. The outlet temperature of mixing devices is determined in the same manner as the combustion devices.

The heat exchangers also employ energy conservation since it is assumed that no heat is lost to the environment. The difference is that the hot and cold streams are not mixed, hence they maintain a given composition. There are two outlet streams, hence two outlet temperatures need to be determined. The effectiveness-NTU [30] method is used to determine the actual temperature changes to both the cold and hot fluid, based on the heat exchanger type, effective heat transfer coefficient and surface area. For a counter flow type heat exchanger:

$$\varepsilon = \frac{1 - \exp[-NTU(1 + C_r)]}{1 + C_r} \quad (8)$$

$$C_r = \frac{C_{min}}{C_{max}} \quad (9)$$

$$NTU = \frac{UA}{C_{min}} \quad (10)$$

$$Q_{max} = C_{min}(T_{in}^{hot} - T_{in}^{cold}) \quad (11)$$

$$Q = \Delta H_{cold} = -\Delta H_{hot} = \varepsilon Q_{max} \quad (12)$$

#### 2.3.2. Compressors and turbine

Practically, compressor and turbine maps are used to determine the operating isentropic efficiencies given the temperature, pressure and flow rates. However, in this particular work, determining the operating conditions of the compressor and turbine is not of interest, since it does not entail the design and selection of appropriate compressors and turbines. In the present power plant, the compressors and turbine already exist. The present work is only interested in retrofitting the existing plant to replace as much combustion with fuel cell processes, so it is desired to maintain "normal" operation of the compressor and turbine. As a result, the inlet conditions to the turbine and compressor, as well as their respective isentropic efficiencies are already known. The only minor difference is that a different amount of fuel will be handled in the hybrid plant than in the standard plant. However, it is assumed that this slight change in flow rate will not significantly affect the isentropic efficiency of the turbine. So in this work, there is no need to determine the isentropic efficiencies since they are already known from analysis of the standard power plant:

$$W = -\Delta H \quad (13)$$

$$\eta_s = \begin{cases} \frac{W}{W_s} & \text{for turbine} \\ \frac{W_s}{W} & \text{for compressor} \end{cases} \quad (14)$$

#### 2.3.3. Solid oxide fuel cell

The SOFC produces DC power via electrochemical processes. The methane is reformed inside the anode compartment, producing hydrogen which is electrolyzed in the SOFC. The following reformation, shift and half cell reactions take place at the respective electrodes:



The operating cell voltage is determined from subtracting all overpotentials (activation, ohmic and concentration) from the standard Nernst potential at the given temperature and pressure:

$$E = -\frac{G_0}{2F} + \frac{RT}{2F} \log \left( \frac{p_{\text{H}_2}}{p_{\text{H}_2\text{O}}} \sqrt{\frac{p_{\text{O}_2}}{p_{\text{atm}}}} \right) \quad (19)$$

$$V_{cell} = E - (\eta_{activation} + \eta_{ohmic} + \eta_{concentration}) \quad (20)$$

$$i = i_0 \left[ \exp \left( \alpha \frac{nF}{RT} \eta_{act} \right) - \exp \left( -(1 - \alpha) \frac{nF}{RT} \eta_{act} \right) \right] \quad (21)$$

$$i_{0,anode} = \gamma_{anode} \frac{p_{\text{H}_2}}{p_{ref}} \frac{p_{\text{H}_2\text{O}}}{p_{ref}} \exp \left( -\frac{E_{act,an}}{RT} \right) \quad (22)$$

$$i_{0,cathode} = \gamma_{cathode} \left( \frac{p_{\text{O}_2}}{p_{ref}} \right)^{1/4} \exp \left( -\frac{E_{act,ca}}{RT} \right) \quad (23)$$

$$\eta_{conc} = \frac{RT}{2F} \log \left( 1 - \frac{i}{i_{lim}} \right) \quad (24)$$

Constants for the ohmic and activation parameters are given elsewhere [31]. The work or power output from the SOFC is the product of total current and cell voltage. The SOFC produces DC power which must be inverted to an AC output. An inverter efficiency of 98% is assumed in this work.

Applying the first law of thermodynamics to the entire fuel cell system, the following equation applies:

$$W_{SOFC} = iV_{cell}A_{SOFC} = -\Delta H_{SOFC} \quad (25)$$

The fuel cell operating temperature in a lumped parameter model is typically taken as the outlet temperature [7] since the inlet gas streams are preheated inside the fuel. This is especially the case in injection tube SOFCs. The SOFC stack is typically designed in such a way as to minimize temperature gradients and hence thermal shock. Thus a fairly uniform spatial temperature distribution is actually achieved in SOFC design. As a result, the outlet temperature (assumed common for both anode and cathode) can be taken as the operating cell temperature. Eq. (25) is used to determine the inlet air temperature required to maintain the predetermined SOFC temperature.

### 2.3.4. Cost functions

The economic analysis of the plant entails the capital costs associated with the SOFC and other related equipment, e.g., heat exchangers, reformers, afterburners, inverters, etc. Presently the cost of SOFC technology is prohibitive, however, the cost analysis in this work is based on projected mass production costs when the technology matures [19]. These projected capital costs are shown below, respectively for the SOFC, inverter, pre-reformer, counter flow heat exchangers, as well as gas turbine components. Capital costs for other auxiliary equipment such as tubing, mixers, valves are taken as 10% of the capital cost of the SOFC.

$$C_{SOFC} = A_{SOFC}(2.96T_{SOFC} - 1907) \quad (26)$$

$$C_{inverter} = 10^5 \left( \frac{W_{SOFC}}{500} \right)^{0.7} \quad (27)$$

$$C_{pre-reformer} = 130 \left( \frac{A_{PR}}{0.093} \right)^{0.78} + 3240(V_{PR})^{0.4} + 21280.5(V_{PR}) \quad (28)$$

$$C_{HX} = 130 \left( \frac{A_{HX}}{0.093} \right)^{0.78} \quad (29)$$

$$C_{SOFC,aux} = 0.1(C_{SOFC}) \quad (30)$$

$$C_{GT} = W_{GT}[1318.5 - 98.328 \ln(W_{GT})] \quad (31)$$

$$C_{comp} = 91,562 \left( \frac{W_{comp}}{445} \right)^{0.67} \quad (32)$$

The thermo-economic model also includes the cost of natural gas ( $C_{gas} = \text{USD } \$3.50 \text{ MBTU}^{-1}$ ) and the cost of water supplied to the fuel cell. The cost analysis is based on a  $n = 10$ -year life cycle with a  $r = 9\%$  rate of interest. The capital costs as well as annual costs are used to determine the life cycle break-even per-unit energy cost. Eq. (33) is used to compute this break-even per-unit energy cost ( $\text{USD } \$ \text{ kWh}^{-1}$ ). Minimizing this energy cost is the design objective in this work:

$$C_{power} = \frac{C_{capital} + 540,168 N_{CH_4}}{56.26 P_{net}} \quad (33)$$

The enthalpy and entropy equations for each species are programmed as user defined functions into MATLAB. The enthalpy and entropy values of each gas species are determined from coefficients used in Ref. [29]. Sub-routines for each component as well as cost functions are then written in MATLAB's programming language. These sub-routines iteratively determine the outlet conditions (temperature and composition) of each component given the inlet conditions. When inlet conditions are unknown, the outlet conditions are initially guessed and iteratively determined. All sub-routines are combined into one plant algorithm which is used to determine all state properties, and hence optimize the hybrid power plant.

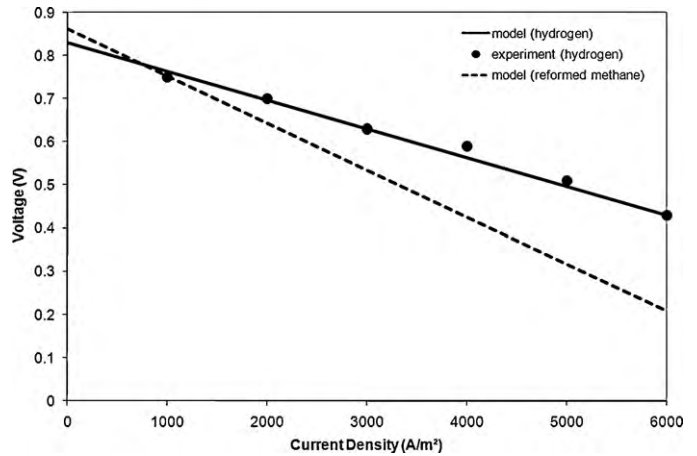


Fig. 2. SOFC model validation.

## 3. Results and discussion

### 3.1. Model validation

The SOFC model is validated using experimental data published in Refs. [21,31,32] (Fig. 2). Experimental data are based on 89%  $H_2$  and 11%  $H_2O$  as the anode fuel, and operation at 1000 °C and 1 atm. The model predictions for this hydrogen cell are within  $\pm 2.3\%$  of the experimental data. The model is then used to predict the SOFC performance for the internally reforming SOFC using methane, also shown in Fig. 2. It predicts that the performance of the cell is diminished because of the lower partial pressure of hydrogen in reformed methane. Unfortunately, data is not readily available for SOFCs using methane or natural gas, thus the internal reformation aspect of the SOFC cannot be validated at this time.

### 3.2. Power plant optimization

The optimization objective is to find the size of the SOFC that minimizes the lifecycle per-unit energy cost. The efficiencies, total power output and energy cost are plotted against the SOFC power in Fig. 3. As expected, the plant power increases linearly as the fuel cell scales up, since the GT maintains an approximately constant power output. The minimum energy cost of  $4.65 \text{ ¢ kWh}^{-1}$  is observed when the SOFC power is 11.0 MW. With indirect coupling, there is a limit to the size of the SOFC that can be coupled

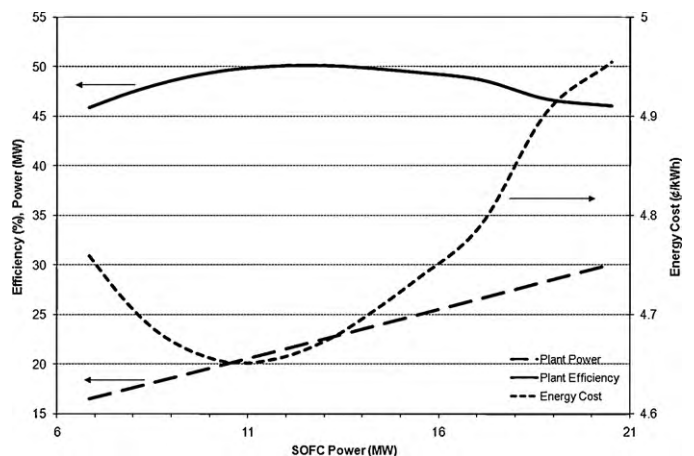


Fig. 3. Power, efficiency and energy cost vs. SOFC power (cell voltage = 0.5 V, anode recycle = 0.6, oxygen/methane ratio = 4).

to the GT, since the turbine outlet stream has a limited heating capacity. If the SOFC is too large, the GT outlet will not be able to properly preheat the SOFC inlet gases. Nevertheless, the plant becomes less economically feasible as the SOFC increases above 11 MW. The plant efficiency peaks at 50.2% at 13 MW SOFC power, however, for an SOFC power of 11 MW, the efficiency is only slightly lower at 49.9%. There is also a lower limit to the size of the SOFC in this configuration. Since the anode outlet (at 1373 K) is recycled, the introduction of this hot stream to the inlet helps to maintain a high SOFC temperature. For small fuel cell stacks (<7 MW), there is the tendency for overheating. This problem can be solved by increasing the air flow rate, however, the performance is found to decrease as the air to fuel ratio increases. Another solution is to remove the heat exchangers at the fuel cell inlet. However, this effectively defeats the purpose of coupling the two power systems. Thus, a small scale SOFC will not achieve the optimum hybrid performance when coupled to a gas turbine in this configuration. An 11 MW SOFC is considered optimal. In this case, the hybrid plant produces 20.6 MW of power.

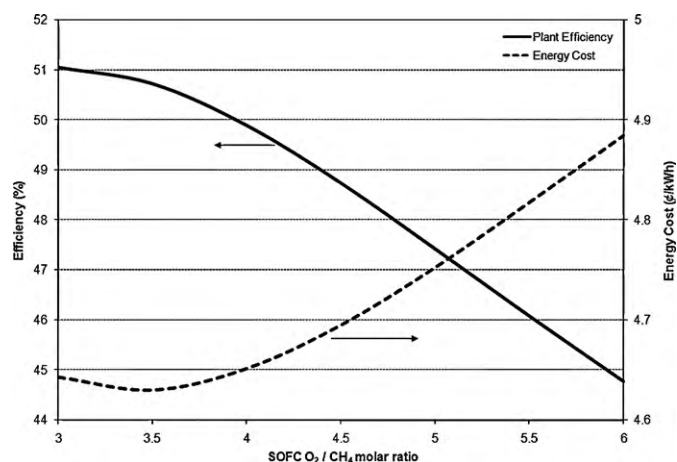
It should be noted that this peak efficiency is well below the 60–70% typically reported for SOFC–GT hybrids. This is because the efficiencies are higher when direct coupling is utilized. With direct coupling, the SOFC and GT use the same working fluid, and as a result the SOFC successfully replaces most of the combustion processes. However, as discussed earlier, direct coupling is not practical for GT power plants already in existence. For such cases indirect coupling is needed, but since only a small amount of combustion is eliminated, the plant efficiencies do not approach that of directly coupled hybrids. Nevertheless, 49.9% efficiency is still considerably high that the 30% efficiency of the standard plant.

Table 1 shows the exergy breakdown of the plant using this optimally sized SOFC. The exergy destruction associated with combustion processes amounts to 20.7% of the net power produced, compared with 111.2% for the standard power plant. However, the SOFC accounts for 19.2%, and the heat exchange and mixing introduced by the coupling accounts for 20.0%. The total exergy destruction is 71.1% of the total plant power, compared with 134.7% for the standard plant. For the hybrid plant, the exergy destruction is distributed among the various components, unlike the standard plant where the combustion device dominates the exergy destruction. These results show that the indirect coupling of the SOFC significantly improves the second law performance of the power plant. The result is that the second law thermal efficiency increases from 28.9% for the standard plant to 48.0% for the hybrid.

Table 2 shows a breakdown of the projected capital and operating costs of the optimized hybrid power plant. The existing GT components (turbine, compressors and combustor) incur a capital cost of \$8.28 M. The cost of the SOFC system is considerably higher at \$16.19 M, while the heat exchangers add a relatively small cost of \$1.60 M. Operating costs include the annual cost of natural gas, estimated at \$4.32 M. Maintenance costs are included in the capital cost of each component. The break-even energy cost is 4.65 ¢ kWh<sup>-1</sup>, which is considerably less than the 5.46 ¢ kWh<sup>-1</sup> energy cost associated with the standard plant, indicating that the hybrid plant produces power in a more cost effective manner than the standard plant.

**Table 2**  
Cost breakdown for the optimized hybrid plant.

System	Cost (USD \$M)	Type
Gas turbine power plant	8.28	Capital
SOFC	16.19	Capital
Heat exchange	1.60	Capital
Gas cost	4.32	Annual
Break-even electricity cost	4.65	



**Fig. 4.** Efficiency and energy cost vs. air/fuel ratio (cell voltage = 0.5 V, anode recycle = 0.6).

### 3.3. Sensitivity analysis

It is of interest to perform a sensitivity analysis on the system to determine the factors that most significantly affect the performance. These factors include the air/fuel ratio, the fraction of anode recycling and the fuel cell voltage. It is known that SOFC performance improves as the temperature increases, thus it is best to operate the SOFC at the highest permissible temperature adhering to material thermal constraints. That value is taken as 1373 K. Simulation has also shown that the most optimum performance occurs when the cell voltage is 0.5 V, the anode recycle fraction is 0.6, and the oxygen/methane molar ratio is 4. Thus these values will be taken as the basis for which the following comparisons are made. Each of these parameters is now varied from their base value to observe the effect on the hybrid plant performance.

Fig. 4 shows the effect of varying the air/fuel ratio in the fuel cell. The energy cost reaches a minimum of 4.63 ¢ kWh<sup>-1</sup> for an oxygen/methane ratio of 3.5. The efficiency on the other hand increases as the oxygen/methane ratio decreases, increasing to over 51% for low air flow rates. Stoichiometrically, the oxygen/methane ratio cannot be lower than 2, however, for oxygen/methane ratios less than 4, the air flow rate is not sufficiently high to regulate the fuel cell temperature. As a result the fuel cell tends to overheat. At higher air flow rates, the decreased performance can be attributed to a higher amount of energy being required to preheat the air entering the SOFC. It is concluded that an oxygen/methane ratio of 4 is ideal. This is also practical in that it ensures sufficient air for proper oxidation of the fuel in both the SOFC and the after-burner.

Fig. 5 shows the effect of varying the fuel cell voltage. It shows that the most optimum performance occurs close to 0.5 V. The energy cost reaches a minimum at approximately 0.47 V while the efficiency peaks at 0.52 V. As the cell voltage increases, although the fuel cell exergy destruction is less, the plant performance decreases mainly because of reduced heat generation in the fuel cell, which decreases the synergistic effect of the hybrid power plant. At lower cell voltages, there is the risk of approaching the limiting current. The plant performance is optimum when the cell is operated at 0.5 V.

Fig. 6 shows the effect of varying the anode recycle fraction. It can be shown theoretically, that for 75% fuel utilization in the SOFC, this anode recycle fraction cannot be lower than 0.58 otherwise there will not be sufficient steam for reformation. Fig. 6 shows that the performance of the hybrid plant improves steadily as the anode recycle fraction decreases. For recycle fractions above 0.75, the SOFC tends to overheat so those results are not shown. These

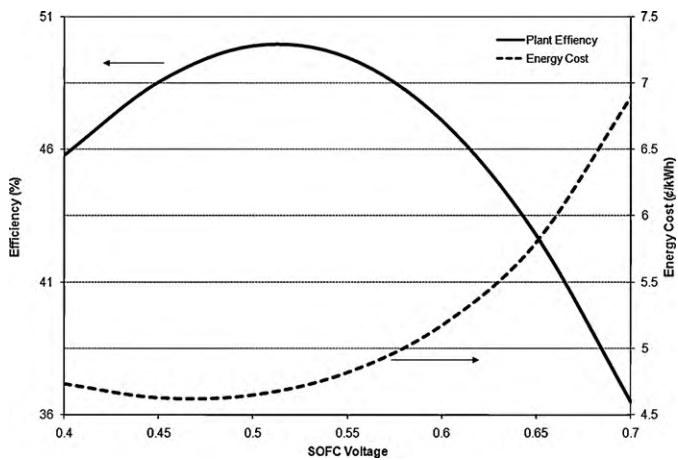


Fig. 5. Efficiency and energy cost vs. SOFC voltage (anode recycle = 0.6, oxygen/methane ratio = 4).

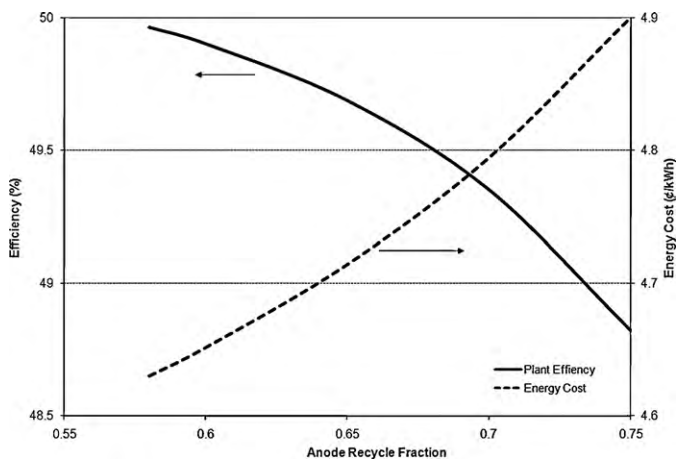


Fig. 6. Efficiency and energy cost vs. anode recycle fraction (cell voltage = 0.5 V, oxygen/methane ratio = 4).

results show that it is ideal to use the lowest permissible fraction of recycling. In this work that value is taken as 0.6.

#### 4. Conclusions

A thermo-economic model was developed and used to optimize an indirectly coupled SOFC–GT hybrid power plant. Indirect coupling was utilized because it offers the most practical coupling of SOFCs to existing GT power plants. Results show that the overall

thermal efficiency can be increased from 30% to 48.0% while the cost of producing power can be reduced from 5.46 to 4.65  $\text{€ kWh}^{-1}$  as a result of the coupling. The most optimum performance was observed when a 11 MW SOFC was used for a total power output of 20.6 MW. Sensitivity analyses also show that for indirectly coupled SOFC–GT hybrid applications, it is preferable to operate the SOFC at a cell voltage of 0.5 V, to utilize low air flow rates (100% excess oxygen), and 60% anode recycling.

#### References

- [1] EG&G Technical Services, Fuel Cell Handbook, 7th ed., US Department of Energy, Morgantown, WV, 2003.
- [2] X. Zhang, S.H. Chan, G. Li, H.K. Ho, J. Li, Z. Feng, J. Power Sources 195 (2010) 685–702.
- [3] K.P. Litzinger, Comparative evaluation of SOFC gas turbine hybrid options, in: Proceedings of the ASME Turbo Expo Conference, Reno, NV, June, 2005.
- [4] D.G.D. Agnew, The design and integration of the rolls royce fuel cell systems 1MW SOFC, in: Proceedings of the ASME Turbo Expo Conference, Reno, NV, June, 2005.
- [5] A. Traverso, M. Pascenti, M.L. Ferrari, R. Bertone, L. Magistri, Hybrid simulation facility based on commercial 100 kW micro gas turbine, in: Proceedings of the ASME Fuel Cell Conference, Irvine, CA, June, 2007.
- [6] A.F. Massardo, F. Lubelli, J. Eng. Gas Turb. Power 122 (2000) 27–35.
- [7] S.H. Chan, C.F. Low, O.L. Ding, J. Power Sources 103 (2002) 188–200.
- [8] P.G. Bavarasad, Int. J. Hydrogen Energy 32 (2007) 4591–4599.
- [9] F. Calise, M.D. d'Accadia, A. Palombo, L. Vanoli, Energy 31 (2006) 3278–3299.
- [10] T.W. Song, J.L. Sohn, T.S. Kim, S.T. Ro, J. Power Sources 158 (2006) 361–367.
- [11] A.V. Akkaya, B. Sahin, H.H. Erdem, Renew. Energy 34 (2009) 1863–1870.
- [12] Y. Haseli, I. Dincer, G.F. Naterer, Int. J. Hydrogen Energy 33 (2008) 5811–5822.
- [13] Y. Haseli, I. Dincer, G.F. Naterer, Thermochim. Acta 480 (2008) 1–9.
- [14] A.V. Akkaya, B. Sahin, H.H. Erdem, Int. J. Hydrogen Energy 33 (2008) 2566–2577.
- [15] W. Burbank Jr., D. Witmer, F. Holcomb, J. Power Sources 193 (2009) 656–664.
- [16] F. Calise, A. Palombo, L. Vanoli, J. Power Sources 158 (2006) 225–244.
- [17] A. Franzoni, L. Magistri, A. Traverso, A.F. Massardo, Energy 33 (2008) 311–320.
- [18] F. Palazzi, N. Autissier, F.M.A. Marechal, M.D. Favrat, Appl. Therm. Eng. 27 (2007) 2703–2712.
- [19] A.M. Arsalis, J. Power Sources 181 (2008) 313–326.
- [20] M. Santin, A. Traverso, L. Magistri, A.F. Massardo, Energy (2009), doi:10.1016/j.energy.2009.06.012.
- [21] F. Calise, M.D. d'Accadia, L. Vanoli, M.R. von Spakovsky, J. Power Sources 159 (2006) 1169–1185.
- [22] S.H. Chan, H.K. Ho, T. Tian, Int. J. Hydrogen Energy 28 (2003) 889–900.
- [23] C. Bao, Y. Shi, C. Li, N. Cai, Q. Su, Int. J. Hydrogen Energy (2009), doi:10.1016/j.ijhydene.2009.05.047.
- [24] X. Zhang, J. Li, G. Li, Z. Feng, J. Power Sources 163 (2006) 523–531.
- [25] R. Kandepu, L. Imsland, B.A. Foss, C. Stiller, Energy 32 (2007) 406–417.
- [26] S.C. Singhal, K. Kendall, High Temperature Solid Oxide Fuel Cells, Elsevier, London, UK, 2003.
- [27] J. Larminie, A. Dicks, Fuel Cell Systems Explained, John Wiley and Sons, Chichester, UK, 2003.
- [28] I. Dincer, M.A. Rosen, Exergy: Energy, Environment and Sustainable Development, Elsevier Science, Oxford, UK, 2007.
- [29] J. Winterbone, Advanced Thermodynamics for Engineers, Butterworth-Heinemann, Oxford, UK, 1996.
- [30] F.P. Incropera, D.P. DeWitt, Fundamentals of Heat and Mass Transfer, John Wiley and Sons, Hoboken, NJ, 2006.
- [31] A.V. Akkaya, Int. J. Energy Res. 31 (2007) 79–98.
- [32] S.C. Singhal, Recent progress in tubular solid oxide fuel cell technology, in: Fifth International Symposium on Solid Oxide Fuel Cells, Aachen, Germany, June, 1997.